

# VVV-WIT-04: an extragalactic variable source caught by the VVV Survey<sup>★</sup>

R. K. Saito<sup>1†</sup>, D. Minniti<sup>2,3,4</sup>, V. D. Ivanov<sup>5</sup>, N. Masetti<sup>6,2</sup>, M. G. Navarro<sup>2,7,3</sup>,  
R. Cid Fernandes<sup>1</sup>, D. Ruschel-Dutra<sup>1</sup>, L. C. Smith<sup>8,9</sup>, P. W. Lucas<sup>9</sup>,  
C. Gonzalez-Fernandez<sup>10</sup>, R. Contreras Ramos<sup>11,3</sup>

<sup>1</sup>Departamento de Física, Universidade Federal de Santa Catarina, Trindade 88040-900, Florianópolis, SC, Brazil

<sup>2</sup>Departamento de Física, Facultad de Ciencias Exactas, Universidad Andres Bello, Av. Fernandez Concha 700, Las Condes, Santiago, Chile

<sup>3</sup>Instituto Milenio de Astrofísica, Santiago, Chile

<sup>4</sup>Vatican Observatory, V00120 Vatican City State, Italy

<sup>5</sup>European Southern Observatory, Karl-Schwarzschild-Str. 2, D-85748 Garching bei Muenchen, Germany

<sup>6</sup>INAF-Osservatorio di Astrofisica e Scienza dello Spazio, Via Piero Gobetti 93/3, I-40129 Bologna, Italy

<sup>7</sup>Dipartimento di Fisica, Università degli Studi di Roma “La Sapienza”, P.le Aldo Moro, 2, I00185 Rome, Italy

<sup>8</sup>Institute of Astronomy, University of Cambridge, Madingley Road, Cambridge, CB3 0HA, UK

<sup>9</sup>Centre for Astrophysics Research, School of Physics, Astronomy and Mathematics, University of Hertfordshire, College Lane, Hatfield AL10 9AB, UK

<sup>10</sup>Institute of Astronomy, University of Cambridge, Madingley Road, Cambridge CB3 0HA, UK 0000-0003-2612-0118

<sup>11</sup>Instituto de Astrofísica, Pontificia Universidad Católica de Chile, Vicuña Mackenna 4860, Macul, Santiago, Chile

Accepted XXX. Received YYY; in original form ZZZ

## ABSTRACT

We report the discovery of VVV-WIT-04, a near-infrared variable source towards the Galactic disk located  $\sim 0.2$  arcsec apart from the position of the radio source PMN J1515-5559. The object was found serendipitously in the near-IR data of the ESO public survey VISTA Variables in the Vía Láctea (VVV). Our analysis is based on variability, multicolor, and proper motion data from VVV and VVV eXtended surveys, complemented with archive data at longer wavelengths. We suggest that VVV-WIT-04 has an extragalactic origin as the near-IR counterpart of PMN J1515-5559. The  $K_s$ -band light-curve of VVV-WIT-04 is highly variable and consistent with that of an Optically Violent Variable (OVV) quasar. The variability in the near-IR can be interpreted as the redshifted optical variability. Residuals to the proper motion varies with the magnitude suggesting contamination by a blended source. Alternative scenarios, including a transient event such as a nova or supernova, or even a binary microlensing event are not in agreement with the available data.

**Key words:** Surveys – Catalogues – Infrared: stars – Stars: individual: VVV-WIT-04 – radio continuum: galaxies – radio continuum: transients

## 1 INTRODUCTION

In the past years, the VISTA Variables in the Vía Láctea (VVV) survey has scanned our Milky Way (MW) galaxy in the near-infrared (near-IR) searching for variable sources (Minniti et al. 2010; Saito et al. 2012). VVV is an European

Southern Observatory (ESO) variability survey, focused on unveiling the 3-dimensional structure of the Milky Way using distance indicators such as pulsating RR Lyrae and Cepheids, as well as red clump stars. In 2016 the complementary VVV eXtended Survey (VVVX, Minniti 2018) started observations, widening the survey area. It is also revisiting the original VVV footprint, thus extending the original time baseline as a result of combining both the VVV and VVVX datasets.

Besides its main goal, VVV has also contributed to the discovery and study of variable sources such as eclipsing bi-

<sup>★</sup> Based on observations taken within the ESO Public Surveys VVV and VVVX, Programme IDs 179.B-2002 and 198.B-2004, respectively.

<sup>†</sup> E-mail: [saito@astro.ufsc.br](mailto:saito@astro.ufsc.br)

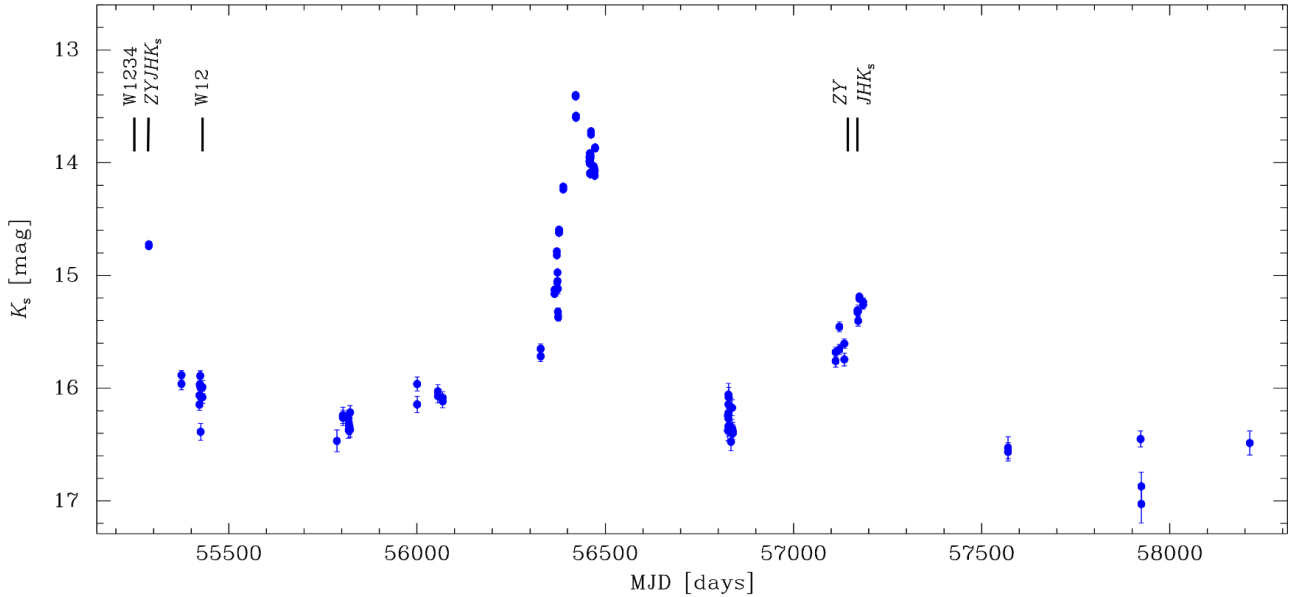


**Figure 1.**  $K_s$ -band light-curve of VVV-WIT-04 combining data from the VVV and VVVX surveys. There is a total of 111 data-points spanning from March 31, 2010 to April 3, 2018. The two epochs of WISE observations as well as the epochs for the multicolour VVV data are marked. “W1234” means WISE observations in the four filters (W1, W2, W3 and W4) while “W12” represents WISE observations only in W1 and W2.

naries, young stellar objects, planetary transits, RR Lyrae and Cepheid variables, etc. Specifically, a search for transient sources such as microlensing events and novae outbursts has resulted in the discovery of a large number of new events in the inner MW (e.g., Saito et al. 2013, 2016; Navarro et al. 2017, 2018). Among the targets found as high-amplitude transient sources in the VVV data, some caught our attention because their behaviour does not seem to fit the currently known classes of stellar variability. We named these targets as “What Is This” (WIT) objects. These rare sources include SN candidates in the MW or behind it (VVV-WIT-01 and VVV-WIT-06, Minniti et al. 2012, 2017) and a possible second example of the “Tabby’s star” (VVV-WIT-07, Saito et al. 2019).

VVV-WIT-04 is a transient source located  $\sim 0.2$  arcsec apart from the position of the radio source PMN J1515–5559 in the inner MW disk (Wright et al. 1994), discovered in a search for large amplitude objects in the VVV data (Saito et al. 2015). VVV observations during years 2010–2013 showed VVV-WIT-04 increasing in brightness by  $\Delta K_s > 2.5$  mag. Based on the VVV  $K_s$ -band light-curve limited to the 2013 season, Saito et al. (2015) suggested that it was a Galactic nova or even a supernova in a galaxy behind the Milky Way.

Here we present an analysis of VVV-WIT-04 based on the VVV/VVVX variability, multicolor, and proper motion data covering 2010–2018. Complementary archive data in the mid/far infrared and radio aided in the analysis and interpretation. We suggest that VVV-WIT-04 is the near-IR counterpart of the radio-source PMN J1515–5559. The variability in the near-IR is consistent with an Optically Violent Variable (OVV), and can be interpreted by the optical variability shifted towards longer wavelengths. Alternative sce-

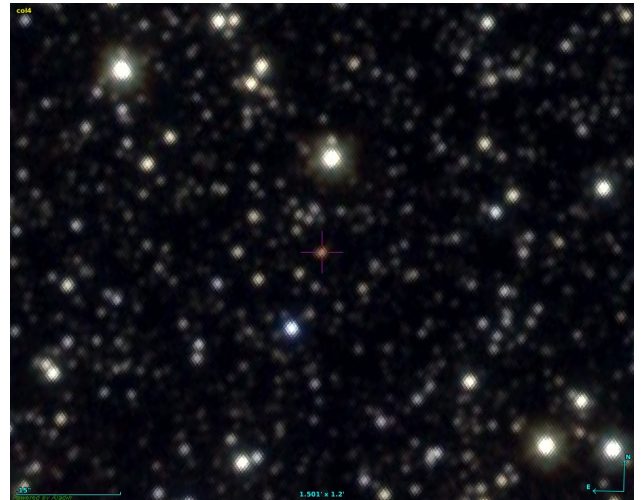


**Figure 2.** VVV  $JHK_s$  false-color image of VVV-WIT-04 area based on observations taken in year 2010 (see Table 1). The field size is  $1.5' \times 1.2'$  and oriented in equatorial coordinates. North is towards the top and East towards the left. The reticle at the centre marks VVV-WIT-04. We note that the object is the reddest source in the field.

narios are also discussed, none of which is fully consistent with the available data.

## 2 OBSERVATIONS AND ARCHIVE DATA

The VVV observational strategy consists in two sets of quasi-simultaneous ZY and  $JHK_s$  photometry, and a variability campaign in the  $K_s$ -band with 50 – 200 epochs car-

**Table 1.** Archive data for VVV-WIT-04. Observations are limited to long wavelengths. The VVV  $K_s$  epochs presented here correspond to the ones observed simultaneously with the  $J$  and  $H$  bands. WISE epochs and magnitudes are mean values over 15 (Feb 2010) and 16 (Aug 2010) observations taken within approximately 1 day interval (see Appendix B). Radio data are in mJy units. Julian dates for radio observations are mean values.

Filter	Survey	$\lambda_C$ [ $\mu\text{m}$ ]	Mag [mag]	Epoch [date (JD)]
$Z$	VVV	0.878	$19.617 \pm 0.083$	Mar 30, 2010 (2455285)
$Z$	VVV	0.878	$20.035 \pm 0.115$	May 03, 2015 (2457145)
$Y$	VVV	1.021	$18.582 \pm 0.048$	Mar 30, 2010 (2455285)
$Y$	VVV	1.021	$18.880 \pm 0.078$	May 03, 2015 (2457145)
$J$	VVV	1.254	$17.374 \pm 0.039$	Apr 01, 2010 (2455287)
$J$	VVV	1.254	$17.843 \pm 0.047$	May 28, 2015 (2457170)
$H$	VVV	1.646	$15.934 \pm 0.030$	Apr 01, 2010 (2455287)
$H$	VVV	1.646	$16.557 \pm 0.047$	May 28, 2015 (2457170)
$K_s$	VVV	2.149	$14.732 \pm 0.016$	Apr 01, 2010 (2455287)
$K_s$	VVV	2.149	$15.318 \pm 0.019$	May 28, 2015 (2457170)
W1	WISE	3.35	$13.130 \pm 0.138$	Feb 20–21, 2010 (2455249)
W1	WISE	3.35	$13.843 \pm 0.423$	Aug 20–22, 2010 (2455430)
W2	WISE	4.60	$12.295 \pm 0.119$	Feb 20–21, 2010 (2455249)
W2	WISE	4.60	$13.881 \pm 0.067$	Aug 20–22, 2010 (2455430)
W3	WISE	11.6	$9.481 \pm 0.206$	Feb 20–21, 2010 (2455249)
W4	WISE	22.1	$7.304 \pm 0.286$	Feb 20–21, 2010 (2455249)

Passband		Frequency	Flux [mJy]	
4.8 GHz	PMN	4.8 GHz	$1990 \pm 99$	June 1990 (2448057)
4.8 GHz	PMN-ATCA	4.8 GHz	$1041 \pm 18$	Nov 9–15, 1992 (2448938)
8.6 GHz	PMN-ATCA	8.6 GHz	$815 \pm 38$	Nov 9–15, 1992 (2448938)
8.6 GHz	VLBI	8.6 GHz	$1463 \pm 225$	Dec 12, 2009 (2455177)

ried out over many years (2010 – 2016). The strategy of the VVVX Survey is similar consisting of  $JHK_s$  photometry plus 3 to 10 epochs in  $K_s$ -band.

VVV-WIT-04 is located in the VVV *tile* d133, towards the Galactic disk. In particular,  $ZY$  data for this tile were collected on Mar 30, 2010 and May 03, 2015 while  $JHK_s$  observations were taken on Apr 01, 2010 and May 28, 2015 (see Table 1). In addition to the colour data, a total of 63  $K_s$ -band observations spanning from Mar 31, 2010 to Apr 28, 2018 were also taken with irregular cadence.

The standard VVV data are based on aperture photometry provided by the Cambridge Astronomical Survey Unit (CASU) on the stacked VVV tile images (see Saito et al. 2012, for details). Due to a high crowding in the inner disk – where VVV-WIT-04 is located – both colour and variability data presented here are based on PSF photometry performed on the VVV images (e.g., Contreras Ramos et al. 2017; Smith et al. 2018), unlike the 2010–2013 VVV CASU data presented in Saito et al. (2015). The  $K_s$ -band light-curve of VVV-WIT-04 combining PSF data from the VVV and VVVX surveys is presented in Fig. 1.

VVV-WIT-04 is located at coordinates RA, DEC (J2000)=15:15:12.69,  $-55:59:32.78$ , corresponding to  $l, b = -37.869, 1.432$  deg. The position coincides within  $\sim 0.2$  arcsec with the radio source PMN J1515–5559 (= LQAC\_228-055\_001, Wright et al. 1994; Souchay et al. 2015; Gattano et al. 2018). Precise coordinates for J1515–5559 from the Very-Long-Baseline Interferometry (VLBI) Source Position Catalogue<sup>1</sup> are RA, DEC (J2000)

= 15:15:12.672880,  $-55:59:32.83821$ , with errors in the coordinates as  $\sigma_{\text{RA}}, \sigma_{\text{DEC}} = 0.67, 0.27$  mas (Petrov et al. 2019, and references therein).

A false-color image of the VVV-WIT-04 area produced from the  $JHK_s$  2010 images is shown in Fig. 2: VVV-WIT-04 appears as a faint point source, much redder than the surrounding field stars. According to the VVV extinction maps (Minniti et al. 2018) the region has a total extinction of  $A_{K_s} = 0.77$  mag, corresponding to  $A_V = 6.52$  mag, assuming the law of Cardelli et al. (1989). These values are similar to those in Schlafly & Finkbeiner (2011), where  $A_K = 0.73$  mag and  $A_V = 6.65$  mag.

An archive search at the VVV-WIT-04 position resulted in few measurements at longer wavelengths. Two sets of observations with Wide-field Infrared Survey Explorer (WISE) were secured on February and August 2010 (Cutri et al. 2012; Cutri & et al. 2013a) the latter being simultaneous with our VVV data. In the following Sections as well as in Table 1 the WISE magnitudes are mean values over a dozen observations taken within approximately 1 day interval by this satellite (see Fig. 5). The complete WISE dataset is presented in the Appendix A. Besides the measurements in the VLBI Source Position Catalogue (Petrov et al. 2019) taken in Dec 2009 at 8.6 GHz, PMN J1515–5559 was also observed by the Parkes-MIT-NRAO (PMN) Survey (Wright et al. 1994) at 4.8 GHz in June 1990, and by the Australia Telescope PMN (ATCA-PMN) Follow-up Survey at 4.8 and 8.6 GHz in Nov 1992 (McConnell et al. 2012).

<sup>1</sup> [http://astrogeo.org/vlbi/solutions/rfc\\_2019a/](http://astrogeo.org/vlbi/solutions/rfc_2019a/)

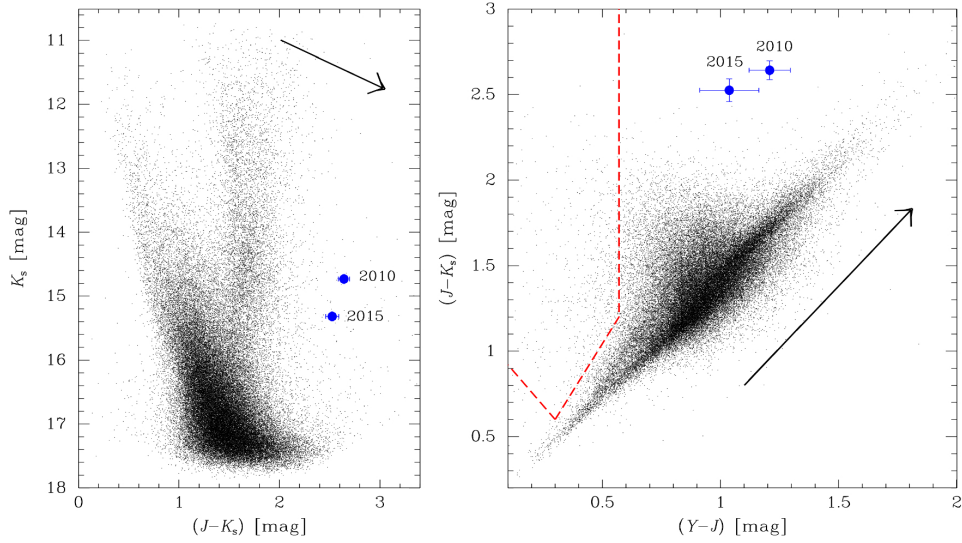


**Figure 3.**  $K_s$  vs.  $(J - K_s)$  CMD (left-panel) and  $(Z - Y)$  vs.  $(J - K_s)$  CCD (right-panel) for stellar sources within 10 arcmin of the target position. The magnitudes and colours of VVV-WIT-04 in year 2010 and 2015 are shown in both panels as blue circles. The reddening vector associated with an extinction of  $A_V = 6.52$  mag (see Section 2), based on the relative extinctions of the VISTA filters, and assuming the (Cardelli et al. 1989) extinction law, is also shown in both panels. In the CCD dashed lines mark the region populated by quasars found behind the Magellanic Clouds using VISTA data (adapted from Ivanov et al. 2016). The colors of VVV-WIT-04 are consistent with a very reddened quasar.

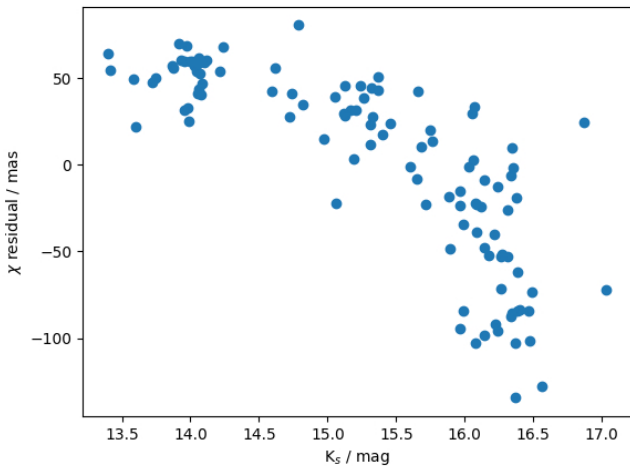


**Figure 4.** Distribution of the residuals to the proper motion as a function of the magnitude for the  $K_s$ -band data. It suggests contamination by a blended source. When VVV-WIT-04 is in the high-stage it dominates the position while the contamination is stronger when VVV-WIT-04 is faint, moving the centroid towards the position of the contaminator.

### 3 DISCUSSION

VVV-WIT-04 was found serendipitously during a search for high amplitude variables in the VVV data (Saito et al. 2013, 2016). As shown in Saito et al. (2015), the  $K_s$ -band light-curve of VVV-WIT-04 covering 2010–2013 seasons is highly variable and increases in brightness by  $\Delta K_s > 2.5$  mag during the late 2012 and the beginning of the 2013 season, peaking at  $K_s = 13.4$  mag on May 2013. After this event, instead

of decreasing steadily as expected for a putative outburst (or even a microlensing event), the 2013–2018 light-curve shows an irregular variability pattern, going fainter than  $K_s = 16$  mag in 2014 and then presenting a second peak on May 2015 at  $K_s = 15.2$  mag. On June 2017 the object is as faint as  $K_s = 17$  mag, thus presenting a total variation of  $\Delta K_s > 3.6$  mag over the nine years of the VVV and VVVX coverage.

The colour of VVV-WIT-04 also varies in time. In 2010,  $(Y - J) = 1.21$  mag and  $(J - K_s) = 2.64$  mag. Assuming the law of Cardelli et al. (1989) and  $A_V = 6.52$  mag,  $(Z - Y)_0 = 0.49$  mag and  $(J - K_s)_0 = 1.58$  mag. Later in 2015,  $(Y - J) = 1.03$  mag and  $(J - K_s) = 2.52$  mag. A  $K_s$  vs.  $(J - K_s)$  colour-magnitude diagram (CMD) and a  $(Y - J)$  vs.  $(J - K_s)$  colour-colour diagram (CCD) for stellar sources within 10 arcmin radii of around the target position are shown in Fig. 3. Both diagrams show that VVV-WIT-04 does not have typical star colors. In fact, the VVV colors of VVV-WIT-04 are in full agreement with a very reddened quasar, similar to the ones found behind the Magellanic Clouds by Ivanov et al. (2016) using VISTA data, when applied the extinction of  $A_V = 6.52$  mag towards the position of VVV-WIT-04 (see Section 2). Its WISE colors are also consistent with an AGN (e.g., Mateos et al. 2012; Maitra et al. 2019).

Proper motions from the VVV Infrared Astrometric Catalogue (VIRAC, Smith et al. 2018) show that the residuals to the proper motion varies as a function of the magnitude for the  $K_s$ -band observations by up to 100 mas, as shown in Fig. 4. That correlation suggests contamination by a blended, faint source. When VVV-WIT-04 is in the high-stage it dominates the target position. On the other hand, when it is faint the contamination is stronger, moving the centroid towards the position of the blended contaminant source.

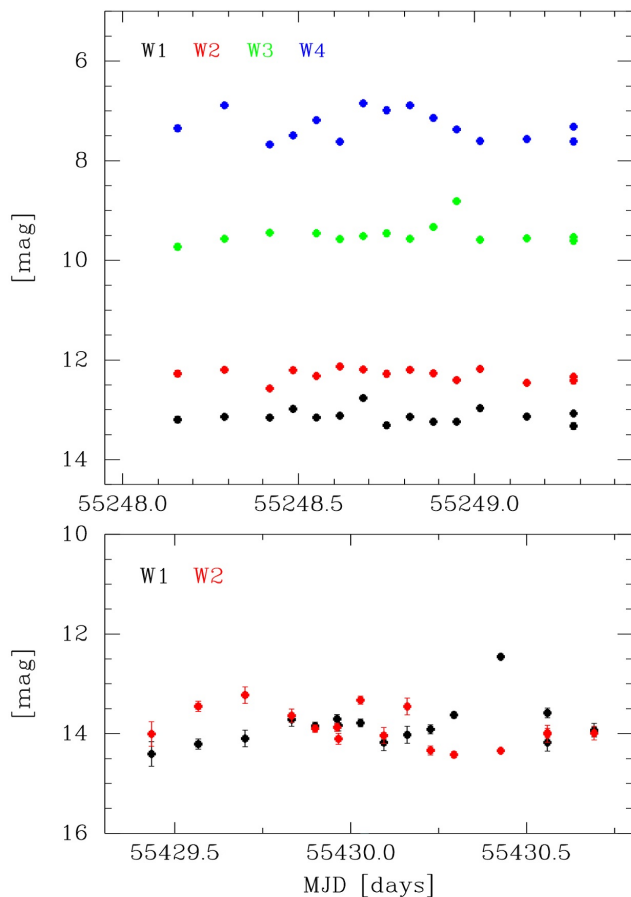


**Figure 5.** WISE light-curves of VVV-WIT-04 within about 1 day coverage. Top panel: Feb 2010 data. Bottom panel: Aug 2010 data. For some data-points, especially in the top panel, the error bars are smaller than the symbols.

The WISE observations also present variations in the mid-IR (see Fig. 5). In Feb 2010 the object is seen at mean magnitude  $W1 = 13.10$  mag with  $(W1 - W2) = 0.84$  mag compared with  $W1 = 13.84$  mag with  $(W1 - W2) = -0.04$  mag in Aug 2010.

#### 4 POSSIBLE INTERPRETATIONS

Quasi-stellar radio sources - Quasars - are luminous active galactic nuclei (AGN). These extragalactic objects are intrinsically blue, but due to local or Galactic absorption, sometimes appear as red(dened) point sources, closely mimicking a distant star. Within the Quasar’s zoo are the Optically Violent Variable (OVV) quasars, which are a type of rare, highly variable quasars, proposed to be unified under the class of Flat Spectrum Radio Quasars (FSRQ). OVV’s are characterized by very rapid variability, high and variable polarization as well as high brightness temperatures (Urry & Padovani 1995). A well studied case is the OVV 3C 279, with multiwavelength coverage over many years (Kartaltepe & Balonek 2007; Patiño-Álvarez et al. 2018, 1990–2002, 2008–2014, respectively). In the optical and near-IR, 3C 279 presents variations as large as 4 mag on different timescales.

Close to the OVV’s are the BL Lac objects, which are also variable AGNs presenting a spectral energy distribution (SED) similar to FSRQs. BL Lacs and OVV’s are blazar sub-types, which embrace all quasars with the relativistic jet closely aligned to the line of sight of the observer. Compared with the OVV’s, BL Lac objects are generally less luminous and present a relatively featureless spectrum, with weak emission or absorption lines. In blazars both optical and near-IR variability time-scales depend on the distance from the emitting region to the central engine and range from months to hours, the latter indicating that the source is compact (Ghisellini et al. 2011a,b, and references therein).

VVV-WIT-04 is a point source located  $\sim 0.20$  arcsec apart from the position of PMN J1515-5559. Catalogued as the quasar LQAC-228-055-001 (Souhay et al. 2015; Gattano et al. 2018), the archive radio data of PMN J1515-5559 are consistent with non-thermal radiation from a compact radio source as expected for an AGN. As discussed in Section 3 (see also Figures 2 and 3) the colour of VVV-WIT-04 is not a typical star colour, but rather it is in agreement with a very reddened quasar (e.g., Mateos et al. 2012; Ivanov et al. 2016; Maitra et al. 2019), leading us to suggest that VVV-WIT-04 has an extragalactic origin as the near-IR counterpart of PMN J1515-5559.

In the scenario, the near-IR counterpart is highly variable in time as shown by our VVV light-curve as well as the WISE archive data. In particular, the VVV light-curve resembles the ones obtained by Patiño-Álvarez et al. (2018, see their Fig. 3) for the OVV 3C 279. However, 3C 279 is observed to vary also at optical wavelengths, as Optically Violent Variable Quasar should behave, while no optical data are available to verify the behaviour of VVV-WIT-04 at shorter wavelengths. The absence of optical data is probably due to the high extinction. In fact, for a galaxy behind the MW, the total extinction as calculated by the VVV maps is probably underestimated.

Our source has an observed magnitude of  $K_s = 16.5$  mag in its “quiescent phase”, which corresponds to a dereddened magnitude of  $K_s \sim 15$  mag, assuming an extinction of  $A_{K_s} = 1.54$  mag (with the caveat cited above). By comparing this magnitude to that of 3C 279 ( $K=10.9$  mag from the 2MASS point source catalog; Cutri, et al. 2003b) we can infer that VVV-WIT-04 is 6.5 times more distant. Based on the WMAP nine-year model cosmology (Hinshaw 2012), and on a redshift of  $z = 0.536$  (Marziani et al. 1996), the luminosity distance to 3C 279 is 3.13 Gpc. Were VVV-WIT-04 to have the same luminosity as this prototypical OVV QSO, its magnitude would imply a redshift of  $z = 2.46$ . Therefore, it is reasonable to assume that the variability we detect in the near infrared could simply be the optical variability shifted towards longer wavelengths due to the recessional velocity of the source.

Previous interpretations of VVV-WIT-04 as a transient event such as a nova or even a supernova (Saito et al. 2015) do not agree with the current data, especially because of the irregular behaviour during seasons 2013–2018 – as example of the secondary peak of  $\Delta K_s \sim 1$  mag observed on May 2015 – since the remnant of a nova or a supernova is expected to decline in brightness slowly and steadily with time. That would not be the first case where a variable quasar is misinterpreted as a high amplitude stellar source. For instance, J004457+4123 (= Sharov 21, Sharov et al. 1998) was first

announced as a remarkable nova in M31 and later confirmed as a background quasar with a strong UV flare (Meusinger et al. 2010).

We have also considered other kinds of sources highly variable in the near-IR. Some microlensing events, for example, can have large amplitudes. The amplitude of a microlensing event is related to the impact parameter (Paczynski 1986), therefore, a considerable increase in the brightness of a source can be explained with this effect. In this case, the curve may resemble a binary microlensing event due to the two most pronounced peaks around MJD~56400 and MJD~57200. To evaluate this scenario we fitted the light-curve using the python Light-curve Identification and Microlensing Analysis (PyLima, Bachelet et al. 2017). The fit does not follow the observational data neither in the base (which is not constant) nor during the increases in brightness. Moreover, colour changes are not expected during microlensing events, contrary to the observed in VVV-WIT-04. For these reasons we disfavor the possible explanation of this object as a microlensing event.

## 5 CONCLUSIONS

We have presented VVV-WIT-04, a variable source identified by the VVV survey towards the Galactic disk at the position of the radio source PMN J1515-5559. Based on VVV/VVVX variability, multicolor, and proper motion data our analysis suggests that VVV-WIT-04 has an extragalactic origin as the near-IR counterpart of the radio-source PMN J1515-5559, with characteristics of an Optically Violent Variable (OVV) quasar. The near-IR variability can be interpreted as the redshifted optical variability. Residuals to the proper motion suggest that VVV-WIT-04 is blended with a nearby source, probably a faint star in the foreground Milky Way disk. Alternative scenarios, including a transient event such as a nova or supernova outburst as proposed by Saito et al. (2015), or even a binary microlensing event have also been discussed and are not in agreement with the currently available data, including the variability pattern and colours, which disfavors all the listed hypotheses.

The absence of spectroscopic information makes difficult to unequivocally classify VVV-WIT-04 among the AGN variable sub-types, since the classification is also based on spectral features. For instance, OVV, BL Lacs or even UltraLuminous InfraRed Galaxies (ULIRGs) could present similar variability behaviour in the optical/near-IR, despite the differences in the luminosity and spectra (e.g., Lonsdale et al. 2006; Ghisellini et al. 2011b; Dexter, & Begelman 2019; Gopal-Krishna et al. 2019).

Compact radio sources are distributed over the whole celestial sphere, including towards the Galactic plane (e.g., Petrov et al. 2019). Similar to VVV-WIT-04 (= PMN J1515-5559), other violent variable near-IR counterparts of radio sources should be present in the database of recent completed (e.g., VVV and UKIDSS-GPS, Lucas et al. 2008) and ongoing (e.g., VVVX) IR multiepoch surveys of the inner Galaxy. A search for high amplitude near-IR variability at the position of radio sources in these surveys should reveal new interesting objects as is the case of VVV-WIT-04.

## ACKNOWLEDGEMENTS

We gratefully acknowledge the use of data from the ESO Public Survey program IDs 179.B-2002 and 198.B-2004 taken with the VISTA telescope, and data products from the Cambridge Astronomical Survey Unit (CASU). This publication makes use of data products from the Wide-field Infrared Survey Explorer, which is a joint project of the University of California, Los Angeles, and the Jet Propulsion Laboratory/California Institute of Technology, funded by the National Aeronautics and Space Administration. R.K.S. acknowledges support from CNPq/Brazil through projects 308968/2016-6 and 421687/2016-9. P.W.L. is supported by STFC Consolidated Grant ST/R000905/1. Support for the authors is provided by the BASAL CONICYT Center for Astrophysics and Associated Technologies (CATA) through grant AFB-170002, and the Ministry for the Economy, Development, and Tourism, Programa Iniciativa Científica Milenio through grant IC120009, awarded to the Millennium Institute of Astrophysics (MAS). D.M. acknowledges support from FONDECYT through project Regular #1170121.

## REFERENCES

- Bachelet, E., Norbury, M., Bozza, V., & Street, R. 2017, *AJ*, 154, 203
- Cardelli, J. A., Clayton, G. C., & Mathis, J. S. 1989, *ApJ*, 345, 245
- Contreras Ramos, R., Zoccali, M., Rojas, F., et al. 2017, *A&A*, 608, A140.
- Cutri, R. M., Wright, E. L., Conrow, T., et al. 2012, Explanatory Supplement to the WISE All-Sky Data Release Products, Cutri, R. M., & et al. 2013, *VizieR Online Data Catalog*, 2328, Cutri R. M., et al., 2003, *yCat*, II/246
- Dexter, J., & Begelman, M. C. 2019, *MNRAS*, 483, L17
- Gattano, C., Andrei, A. H., Coelho, B., et al. 2018, *A&A*, 614, A140
- Ghisellini, G., Tagliaferri, G., Foschini, L., et al. 2011, *MNRAS*, 411, 901
- Ghisellini, G., Tavecchio, F., Foschini, L., et al. 2011, *MNRAS*, 414, 2674
- Gopal-Krishna, Britzen, S., & Wiita, P. 2019, *arXiv e-prints*, arXiv:1906.11339
- Hinshaw, G. 2012, American Astronomical Society Meeting Abstracts #220 220, 504.03
- Ivanov, V. D., Cioni, M.-R. L., Bekki, K., et al. 2016, *A&A*, 588, A93
- Kartaltepe, J. S., & Balonek, T. J. 2007, *AJ*, 133, 2866
- Lonsdale, C. J., Farrah, D., & Smith, H. E. 2006, *Astrophysics Update* 2, 285
- Lucas, P. W., Hoare, M. G., Longmore, A., et al. 2008, *MNRAS*, 391, 136
- Maitra, C., Haberl, F., Ivanov, V. D., Cioni, M.-R. L., & van Loon, J. T. 2019, *A&A*, 622, A29
- Mateos, S., Alonso-Herrero, A., Carrera, F. J., et al. 2012, *MNRAS*, 426, 3271
- Marziani, P., Sulentic, J. W., Dultzin-Hacyan, D., et al. 1996, *ApJS*, 104, 37
- McConnell, D., Sadler, E. M., Murphy, T., & Ekers, R. D. 2012, *MNRAS*, 422, 1527
- Meusinger, H., Henze, M., Birkle, K., et al. 2010, *A&A*, 512, A1
- Minniti, D., Lucas, P. W., Emerson, J. P., et al. 2010, *New Astron.*, 15, 433

Minniti, D., Lucas, P. W., Cross, N., et al. 2012, *The Astronomer’s Telegram*, 4041,  
Minniti, D., Saito, R. K., Forster, F., et al. 2017, *ApJ*, 849, L23  
Minniti, D. 2018, in *The Vatican Observatory, Castel Gandolfo: 80th Anniversary Celebration* (ed. G. Gionti, S.J., & J.-B. Kikwaya Eluo, S.J). *Astrophysics and Space Science Proceedings*, 51, 63  
Minniti, D., Saito, R. K., Gonzalez, O. A., et al. 2018, *A&A*, 616, A26  
Navarro, M. G., Minniti, D., & Contreras Ramos, R. 2017, *ApJ*, 851, L13  
Navarro, M. G., Minniti, D., & Contreras-Ramos, R. 2018, *ApJ*, 865, L5  
Paczynski, B. 1986, *ApJ*, 304, 1  
Patiño-Álvarez, V. M., Fernandes, S., Chavushyan, V., et al. 2018, *MNRAS*, 479, 2037  
Petrov, L., de Witt, A., Sadler, E. M., Phillips, C., & Horiuchi, S. 2019, *MNRAS*, 485, 88  
Schlafly, E. F., & Finkbeiner, D. P. 2011, *ApJ*, 737, 103  
Saito, R. K., Hempel, M., Minniti, D., et al. 2012, *A&A*, 537, A107  
Saito, R. K., Minniti, D., Angeloni, R., et al. 2013, *A&A*, 554, A123  
Saito, R. K., da Silva, M. V., Melo, I. S., et al. 2015, *The Astronomer’s Telegram*, 8456,  
Saito, R. K., Minniti, D., Catelan, M., et al. 2016, *The Astronomer’s Telegram*, 8602,  
Saito, R. K., Minniti, D., Ivanov, V. D., et al. 2019, *MNRAS*, 482, 5000  
Sharov, A. S., Alksnis, A., Nedialkov, P. L., et al. 1998, *Astronomy Letters*, 24, 445  
Souhay, J., Andrei, A. H., Barache, C., et al. 2015, *A&A*, 583, A75  
Smith, L. C., Lucas, P. W., Kurtev, R., et al. 2018, *MNRAS*, 474, 1826  
Smith, L., et al. 2018, in preparation  
Sutherland, W., Emerson, J., Dalton, G., et al. 2015, *A&A*, 575, A25  
Urry, C. M., & Padovani, P. 1995, *PASP*, 107, 803  
Wright, A. E., Griffith, M. R., Burke, B. F., et al. 1994, *The Astrophysical Journal Supplement Series*, 91, 111.

**APPENDIX A: VVV-WIT-04  $K_S$ -BAND DATA**

Here we present the PSF  $K_S$ -band data-points of VVV-WIT-04 available from VVV/VVVX and used to build the light-curve presented in Fig. 1. There is a total of 111 data-points spanning from March 31, 2010 to April 3, 2018. The data-point number of data-points (111) is larger than the observed epochs (63) because the PSF photometry is performed on the individual VISTA *pawprint* images instead of on the final VISTA *tile* image (Saito et al. 2012; Sutherland et al. 2015).

MJD (days)	$K_S$ -band (mag)	MJD (days)	$K_S$ -band (mag)
55287.2971	14.739 ± 0.016	56459.0313	13.974 ± 0.010
55287.2978	14.725 ± 0.014	56459.0714	13.980 ± 0.013
55374.1623	15.884 ± 0.041	56459.0866	13.917 ± 0.015
55374.1627	15.962 ± 0.053	56459.0869	13.998 ± 0.010
55422.0077	16.145 ± 0.052	56460.0773	14.089 ± 0.012
55422.0081	16.063 ± 0.054	56460.0777	14.101 ± 0.011
55423.0662	15.965 ± 0.050	56461.1928	13.954 ± 0.013
55423.0666	15.968 ± 0.050	56461.1932	13.934 ± 0.011
55424.0597	15.890 ± 0.045	56462.2526	13.750 ± 0.011
55424.0601	15.988 ± 0.047	56462.2530	13.722 ± 0.010
55425.0361	16.387 ± 0.075	56469.1893	14.031 ± 0.012
55425.0366	16.078 ± 0.056	56469.1897	14.058 ± 0.011
55430.0372	15.991 ± 0.059	56470.1297	14.046 ± 0.011
55430.0377	16.080 ± 0.054	56470.1301	14.051 ± 0.010
55787.1163	16.468 ± 0.098	56471.0304	14.062 ± 0.013
55803.0393	16.262 ± 0.068	56471.0308	14.071 ± 0.013
55803.0397	16.240 ± 0.072	56472.0554	14.073 ± 0.016
55817.9926	16.372 ± 0.071	56472.0730	14.115 ± 0.011
55817.9929	16.267 ± 0.067	56472.0734	14.071 ± 0.014
55818.9870	16.310 ± 0.068	56473.0201	13.865 ± 0.012
55818.9874	16.315 ± 0.086	56473.0205	13.873 ± 0.015
55819.9880	16.342 ± 0.069	56826.0025	16.243 ± 0.095
55819.9884	16.338 ± 0.065	56826.0029	16.377 ± 0.089
55822.0042	16.368 ± 0.067	56826.9796	16.144 ± 0.076
55822.0047	16.215 ± 0.060	56826.9800	16.268 ± 0.086
56000.3317	16.144 ± 0.072	56827.0046	16.342 ± 0.084
56000.3320	15.963 ± 0.062	56827.0050	16.220 ± 0.071
56055.3022	16.028 ± 0.060	56827.0927	16.057 ± 0.100
56055.3026	16.070 ± 0.059	56827.9883	16.083 ± 0.091
56068.2887	16.116 ± 0.056	56827.9887	16.333 ± 0.093
56068.2892	16.085 ± 0.055	56834.0357	16.475 ± 0.080
56328.3548	15.651 ± 0.044	56837.0159	16.356 ± 0.078
56328.3551	15.717 ± 0.049	56837.0163	16.174 ± 0.071
56365.2609	15.163 ± 0.023	56838.9694	16.381 ± 0.078
56365.2613	15.127 ± 0.028	56838.9698	16.400 ± 0.077
56371.3482	14.820 ± 0.018	57112.1651	15.680 ± 0.042
56371.3486	14.787 ± 0.020	57112.1657	15.759 ± 0.055
56372.2801	15.060 ± 0.032	57122.1988	15.456 ± 0.044
56372.2805	15.123 ± 0.031	57122.1992	15.656 ± 0.045
56373.2215	15.050 ± 0.024	57135.1337	15.745 ± 0.056
56373.2219	14.974 ± 0.023	57135.1341	15.605 ± 0.041
56374.2747	15.117 ± 0.048	57170.1658	15.327 ± 0.019
56374.2751	15.323 ± 0.034	57170.1667	15.310 ± 0.017
56375.2302	15.365 ± 0.034	57172.0094	15.403 ± 0.047
56375.2306	15.370 ± 0.033	57172.0098	15.315 ± 0.052
56377.1707	14.595 ± 0.018	57175.0081	15.189 ± 0.023
56377.1714	14.621 ± 0.024	57175.0086	15.206 ± 0.023
56388.4126	14.214 ± 0.013	57184.9903	15.236 ± 0.037
56388.4130	14.236 ± 0.017	57184.9907	15.260 ± 0.038
56421.3793	13.412 ± 0.010	57570.2188	16.528 ± 0.096
56421.3797	13.401 ± 0.011	57570.2192	16.565 ± 0.081
56422.3114	13.600 ± 0.011	57922.1606	16.451 ± 0.071
56422.3118	13.585 ± 0.015	57924.1200	17.028 ± 0.168
56458.1027	13.952 ± 0.011	57924.1204	16.871 ± 0.126
56458.1031	13.988 ± 0.009	58212.3241	16.486 ± 0.106
56459.0309	14.009 ± 0.011		

**APPENDIX B: WISE DATA**

This paper has been typeset from a  $\text{\TeX}/\text{\LaTeX}$  file prepared by the author.

MJD (days)	W1 (mag)	W2 (mag)	W3 (mag)	W4 (mag)
55248.1549	13.198 ± 0.066	12.275 ± 0.055	9.729 ± 0.121	7.350 ± 0.418
55248.2873	13.141 ± 0.055	12.197 ± 0.054	9.566 ± 0.112	6.889 ± 0.220
55248.4196	13.156 ± 0.047	12.572 ± 0.091	9.444 ± 0.121	7.674 ± 0.448
55248.4857	12.983 ± 0.061	12.204 ± 0.066	—	7.493 ± 0.343
55248.5519	13.154 ± 0.054	12.321 ± 0.079	9.456 ± 0.106	7.187 ± 0.348
55248.6181	13.119 ± 0.041	12.130 ± 0.035	9.573 ± 0.133	7.619 ± 0.428
55248.6842	12.764 ± 0.045	12.189 ± 0.053	9.513 ± 0.114	6.848 ± 0.228
55248.7505	13.311 ± 0.065	12.277 ± 0.057	9.457 ± 0.095	6.988 ± 0.240
55248.8165	13.141 ± 0.055	12.197 ± 0.054	9.566 ± 0.112	6.889 ± 0.220
55248.8828	13.241 ± 0.056	12.268 ± 0.063	9.330 ± 0.112	7.143 ± 0.339
55248.9490	13.239 ± 0.050	12.403 ± 0.051	8.813 ± 0.395	7.372 ± 0.469
55249.0151	12.968 ± 0.046	12.180 ± 0.043	9.587 ± 0.118	7.605 ± 0.480
55249.1474	13.136 ± 0.041	12.459 ± 0.059	9.558 ± 0.128	7.566 ± 0.491
55249.2797	13.326 ± 0.067	12.411 ± 0.077	9.605 ± 0.112	7.614 ± 0.413
55249.2798	13.074 ± 0.038	12.337 ± 0.063	9.533 ± 0.118	7.318 ± 0.386
55429.4337	14.407 ± 0.245	14.006 ± 0.292	—	—
55429.5660	14.208 ± 0.103	13.452 ± 0.116	—	—
55429.6984	14.098 ± 0.166	13.225 ± 0.095	—	—
55429.8307	13.716 ± 0.134	13.639 ± 0.186	—	—
55429.8967	13.848 ± 0.077	13.898 ± 0.244	—	—
55429.9628	13.705 ± 0.085	13.872 ± 0.308	—	—
55429.9630	13.836 ± 0.108	14.104 ± 0.212	—	—
55430.0290	13.785 ± 0.079	13.328 ± 0.136	—	—
55430.0951	14.178 ± 0.160	14.037 ± 0.253	—	—
55430.1614	14.023 ± 0.170	13.454 ± 0.121	—	—
55430.2274	13.912 ± 0.090	14.336 ± 0.266	—	—
55430.2937	13.626 ± 0.061	14.422	—	—
55430.4260	12.456	14.342 ± 0.337	—	—
55430.5581	13.583 ± 0.098	13.987 ± 0.290	—	—
55430.5583	14.177 ± 0.172	14.003 ± 0.239	—	—
55430.6904	13.931 ± 0.136	13.990	—	—